Premixed flame propagation between two closely spaced parallel plates

D. Fernández-Galisteo*, J. Gross**, V.N. Kurdyumov*, and P.D. Ronney**

*Department of Energy, CIEMAT. Avda. Complutense 40, 28040. Madrid. Spain
**Department of Aerospace and Mechanical Engineering, University of Southern California, Los Angeles, CA 90089-1453. USA

Abstract

The propagation of slow quasi-isobaric premixed flames between two closely spaced parallel and adiabatic plates is investigated numerically with the use of a quasi-2D formulation based on an averaging of the flow quantities across the direction perpendicular to the plates. The formulation arises when the ratio of the plates separation to the flame thickness becomes small, that is, for values of the Peclet number, $Pe = h/\delta_T \ll 1$. Front shapes and propagation rates are computed based on this formulation to capture the effect of the intrinsic instability mechanisms.

1 Introduction

It is well-known that hydrodynamic instabilities, that do not depend on flame structure, can wrinkle the flame front and modify the overall propagation rates, although the gas flow remains laminar. These instabilities can be enumerated as the Darrieus-Laundau (DL) instability (due to thermal expansion), the Rayleigh-Taylor (RT) instability (due to buoyancy effect), and the Saffman-Taylor (ST) instability (due to viscosity contrast across the flame), the latter showing only considerable effects in very confined flows. Another important instability mechanism, independent of the flame-fluid interaction, is the diffusive-thermal (DT) instability. In this case, when the effective Lewis number, Le, which measures the unequal rates of species diffusion and heat conduction, is less than a critical value close to unity, the planar laminar flame becomes unstable to cellular structures [1].

Joulin and Sivashinsky [2] expanded the models based on the theory of infinitely thin flame, where burned and unburned region are separeted by a discontinuity, in order to investigate the effect of losses of momentum and heat into the intrinsic instabilities. For that purpose, they considered a premixed flame propagating between parallel plates (also known as Hele-Shaw cell), obtaining a dispersion relation for the growth rate of these instabilities. However, the DT instability was not able to be incorporated in this model due to its limitation. Recently, Kang et al. [3, 4] investigated the effect of heat and momemtum losses in the intrinsic flame instabilities by using a complete 2D numerical simulations of the Navier-Stokes equations and the conservation equations for the species with a one-step irreversible reaction,

Correspondence to: d.galisteo@ciemat.es

also in a Hele-Shaw cell configuration. The ST instability mechanism was incorporated when including the viscous force in the direction perpendicular to the plates in the 2D formulation.

The present work shows a quasi-2D formulation, that emerges in the limit of very close plates, capable of capturing the effect of the intrinsic instability mechanisms on the front shapes and propagation rates. The adopted approach is an extension of recent studies based on the limit of narrow channels [5, 6].

2 Formulation

Consider a premixed flame that propagates between two closely spaced parallel and adiabatic plates. The premixed flame is modelled with an irreversible one-step kinetics, $F + O \rightarrow P$, where F, O and P stand for the fuel, the oxidant and the products, respectively. In the formulation, we consider a mixture lean in fuel, so the oxidant, in excess, remains nearly constant.

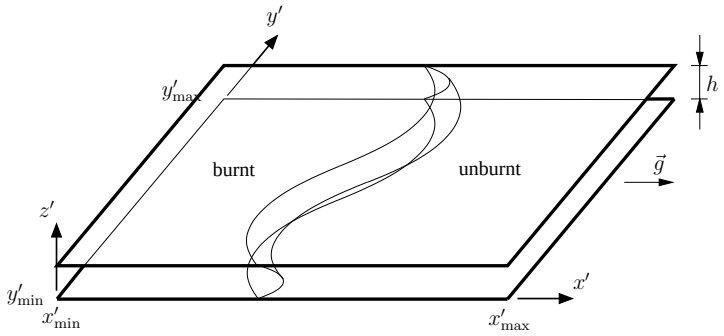

Figure 1: Sketch of the Hele-Shaw cell with a curved flame propagating from the left to the right between two parallel plates with a cell gap h.

If the speed S_L and the thermal thickness δ_T of a planar adiabatic flame are used as the reference scales for an appropiate non-dimensionalization, where $\delta_T = \mathcal{D}_T/S_L$, and the state of the fresh unburnt mixture for density ρ_u, temperature T_u, and fuel mass fraction Y_{F_u} are introduced, the dimensionless variables become

$$x = x'/\delta_T, \qquad y = y'/\delta_T, \qquad z = z'/h, \qquad t = S_L t'/\delta_T,$$

$$u = u'/S_L, \qquad v = v'/S_L, \qquad w = w'/(Pe\, S_L),$$

$$\rho = \rho'/\rho_u, \qquad p = p'\, Pe^2/(12\, Pr\, \rho_u S_L^2), \qquad G = g'\delta_T\, Pe^2/(12\, Pr\, S_L^2),$$

$$\theta = (T' - T_u)/(T_a - T_u), \qquad Y = Y_F/Y_{F_u},$$

where the prime $'$ denotes a dimensional value. Pr corresponds with the Prandtl number, p is the reduced kinematic pressure, G is the reduced gravity field in the direction of the flame propagation, and $T_a = T_u + QY_{F_u}/c_p$ is the adiabatic temperature, with Q being the heat of combustion per unit mass fuel, and c_p the specific heat of the mixture at constant pressure, taken as a constant value in what follows.

The ratio of the plates separation to the flame thickness is denoted as the Peclet number, $Pe = h/\delta_T$. In the limit of two closely spaced plates, $Pe \ll 1$, all variables can be expanded in power of Pe, according to $f = f_0 + Pe^2\, f_1 + \mathcal{O}(Pe^4)$, where f stands for the temperature θ, mass fraction Y, density ρ,

pressure p, and the velocity components u, v, and w. Following the above procedure and making use of the adiabatic condition in the plates, we obtain, at first order, the following equations

$$\rho\frac{\partial\theta}{\partial t}+\rho U_x\frac{\partial\theta}{\partial x}+\rho U_y\frac{\partial\theta}{\partial y}=\nabla\cdot(\mu\nabla\theta)+\omega, \tag{1}$$

$$\rho\frac{\partial Y}{\partial t}+\rho U_x\frac{\partial Y}{\partial x}+\rho U_y\frac{\partial Y}{\partial y}=\frac{1}{Le}\nabla\cdot(\mu\nabla Y)-\omega, \tag{2}$$

where

$$\omega(\theta,Y)=\frac{\beta^2}{2s_L^2Le}\frac{(1+\gamma)^{2-\sigma}}{(1+\gamma\theta)^2}\,Y\exp\left\{\frac{\beta(\theta-1)}{1+[\gamma/(1+\gamma)](\theta-1)}\right\}.$$

$\beta=E(T_a-T_u)/\mathcal{R}T_a^2$ is the Zel'dovich number, $\gamma=(T_a-T_u)/T_u$ is the heat release parameter, Le stands for the Lewis number, and σ corresponds to the exponent of the temperature-dependent viscosity coeficient $\mu=(1+\gamma\theta)^\sigma$. The reduced planar flame speed $s_L=S_L/(S_L)_{asp}$ is introduced for convenience, with the asymptotic value being $(S_L)_{asp}=\sqrt{2Le\mathcal{B}\rho_u\mathcal{D}_{T_u}\lambda_b/(\beta^2\lambda_u)}\;(\rho_b/\rho_u)\exp(-E/2\mathcal{R}T_a)$. Herein, $\mathcal{B}$ is the frequency factor, $\mathcal{D}_{T_u}$ is the value of the thermal diffusivity in the unburnt condition, and λ_u, λ_b, and ρ_b are the values of the thermal conductivity and density in the unburnt and burnt conditions, respectively. E and $\mathcal{R}$ stands for the activation energy and the universal gas constant, respectively.

The problem is completed with the reduced Darcy's law for the z-averaged velocity

$$U_x\,\vec{e}_x+U_y\,\vec{e}_y=\left(\int_0^1 u\,\mathrm{d}z\right)\vec{e}_x+\left(\int_0^1 v\,\mathrm{d}z\right)\vec{e}_y=-\frac{1}{\mu}(\nabla p-\rho G\vec{e}_x), \tag{3}$$

the Laplacian equation for the pressure field

$$\Delta p-(1+\sigma)G\frac{\partial\rho}{\partial x}+\frac{\sigma}{\rho}\nabla\rho\cdot\nabla p=-\gamma\mu\left[\nabla\cdot(\mu\nabla\theta)+\omega\right], \tag{4}$$

and the equation of state

$$\rho=1/(1+\gamma\theta). \tag{5}$$

The combustion field is obtained finally by solving the Eqs. (1)-(5) together with the corresponding boundary conditions.

3 Numerical computations and results

The system of equations was discretized using a first order in time and a second order in space finite differences. Time-dependent computations were carried out in a domain large enough, typically with size of 200×100, to capture correctly the wrinkled flame structures. The cell size $\Delta=\Delta x=\Delta y$ was varied in an uniform grid between 0.2 and 0.4, that is, allowing about 4 to 6 points within the reaction zone. Periodic boundary conditions were used in the transverse boundaries

$$\begin{aligned}\theta(x,y_{\min})&=\theta(x,y_{\max}), & Y(x,y_{\min})&=Y(x,y_{\max}),\\ U_x(x,y_{\min})&=U_x(x,y_{\max}), & U_y(x,y_{\min})&=U_y(x,y_{\max}).\end{aligned} \tag{6}$$

The pressure at the left side was taken as constant and equal to the ambient pressure, and the state of the mixture assumed uniform for simplicity

$$x=x_{\min}: \qquad p=0, \quad \partial\theta/\partial x=\partial Y/\partial x=0. \tag{7}$$

At the right side zero velocity was impossed, together with uniformity of the state of the mixture

$$x = x_{\max}: \quad U_x = U_y = 0, \quad \partial\theta/\partial x = \partial Y/\partial x = 0. \tag{8}$$

The mixture was ignited with three hot spot (where the temperature follows a Gaussian distribution) at the left side in the points $(x, y) = (0, 0), (0, 50)$, and $(0, 100)$. As shown in Figure 4, the first stage corresponds with an acceleration due to thermal expansion, following an steady/unsteady flame propagation, where cell splitting of merging can occur. In the final stage the frame front speed decreases due to the nearness of the end-wall effect. There is a relation between the front speed S_T and the total burning rate $\Omega = (\int_{x_{\min}}^{x_{\max}} \int_{y_{\min}}^{y_{\max}} \omega \, \mathrm{d}x \, \mathrm{d}y)/L_y$, where L_y is the length in the y direction. In the case of steady propagation the solution is independent to translation and one can integrate the Eq. 2 in a reference frame moving at S_T. Using the boundary conditions (6)-(8) one finds that $\Omega = S_T/S_L$. The reduced front speed S_T/S_L is then calculated following this procedure to characterize the flame front propagation velocity.

The effects of buoyancy, viscosity contrast or differential diffusion on the flame wrinkling was studied separately. The case in Figure 2c) with $Le = 1$, $\beta = 10$, $\gamma = 5$, $\sigma = 0$, and $G = 0$ is used as the baseline calculation. It evolves to a steady propagation. This case exhibits flame wrinkles only due to the DL mechanism, which propagate at velocities about 1.5 times faster than the planar flame velocity; see Figure 4. Figures 2d) - 2e) show the stabilizing effect of flames propagating in the direction of the gravity $(G > 0)$. Numerical computations revealed a stable planar flame front propagation for values of $G \gtrsim 5$ in the case of $Le = 1$, indicating that the RT mechanism is competing with the DL instability. Flame wrinkles increase for larger negative values of G, as in the classical instability theory, see Figures 2a) - 2b).

The Figure 3a) depicts the effect of the viscosity contrast, included through the parameter $\sigma = 0.7$. This effect changes the number of waves accommodated in the vertical domain. The main effect is an increase in the front speed with values of 2 times the planar flame velocity (see Figure 4), larger than the baseline case. When the value of Le is decreased the DT instability mechanism is introduced in the computations. The Figure 3b) shows cell formation patterns for $Le = 0.3$. This case shows an unsteady propagation with lateral movements and large values of the flame speed of the order of 7 times the planar flame speed; see Figure 4. The results are in qualitatively good agreement with the structures found in recent experiments of very lean hydrogen mixtures [7].

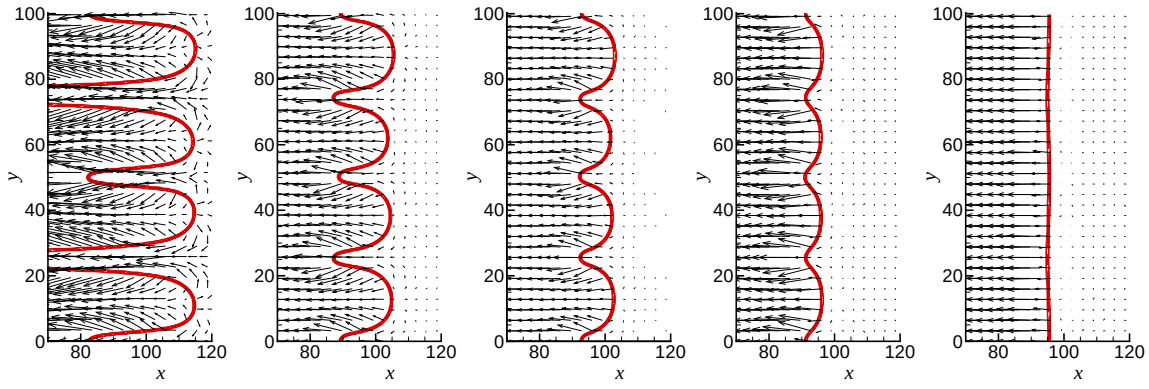

(a) $G = -10$ (b) $G = -2$ (c) $G = 0$ (d) $G = 2$ (e) $G = 5$

Figure 2: Flame fronts represented by the reaction rate contours and the flow velocity vectors calculated for $Le = 1$, $\beta = 10$, $\gamma = 5$, $\sigma = 0$, with increasing values of G (upward propagation for $G < 0$ and downward propagation for $G > 0$).

Finally, in Figure 4 is plotted the values of the front speed for five different cases. In the case $G = 2$, the front speed reaches a steady propagation with $S_T/S_L \approx 1.1$. This is due to the small amplitude of the curved flames compared to the baseline case $G = 0$. The reverse is also true for $G = -2$. In the case $Le = 0.3$ the front speed shows large values, even when the value of γ was reduced to 2.5, due to the cell structures formed. The effect of the viscosity contrast was to increase the front speed up to 30% with respect to the baseline case.

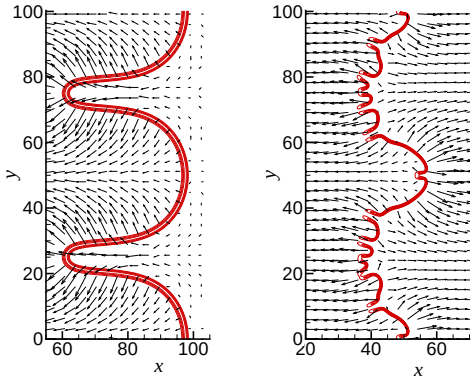

(a) $Le = 1, \sigma = 0.7$ (b) $Le = 0.3, \sigma = 0$

Figure 3: Flame fronts represented by the reaction rate contours and the flow velocity vectors calculated for a) $Le = 1$, $\beta = 10$, $\gamma = 5$, $\sigma = 0.7$, $G = 0$ and b) $Le = 0.3$, $\beta = 10$, $\gamma = 2.5$, $\sigma = 0$, $G = 0$.

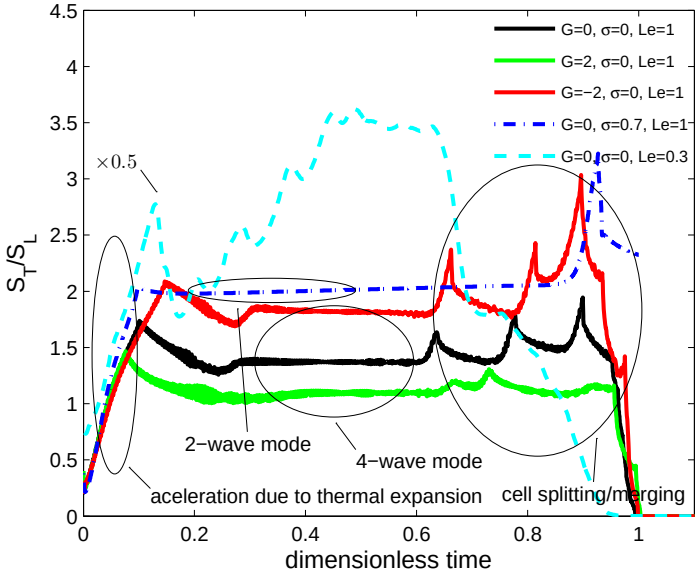

Figure 4: The reduced front speed with the dimensionless time for 5 cases. Solid curves: (centre) for $G = 0$, $\sigma = 0$, $Le = 1$; (down) for $G = 2$, $\sigma = 0$, $Le = 1$; (up) for $G = -2$, $\sigma = 0$, $Le = 1$. Dashed curve: for $G = 0$, $\sigma = 0$, $Le = 0.3$. Dot-dashed curve: for $G = 0$, $\sigma = 0.7$, $Le = 1$.

4 Conclusions and future work

In the limit of two closely spaced parallel plates, the Peclet number, $Pe = hS_L/\mathcal{D}_T$, based on the laminar flame velocity, is used as a parameter of expansion to obtain a simplified model that allows the study of flame instabilities in confined flows. Time-dependent computations with only the DL mechanism included results in wrinkled flame structures. They compete with the RT mechanism when $G > 0$ and are able to stabilize the flame wrinkles to planar flame fronts for a sufficently large positive value of G. The DT instability modifies the flame wrinkles through cell formation, increasing significantly the front speed. The front becomes unsteady with lateral movements. The effect of the ST instability mechanism is introduced through the parameter σ. For the typical values of $\sigma = 0.7$ the calculations show an increase of about 30% in the front speed with respect to the baseline case. The number of waves accommodated in the domain is also different.

The validity of the results in the limit $Pe \ll 1$ needs to be checked with 3D computations, where the effect of the curvature in the third coordinate z plays a role.

References

[1] G. I. Sivashinsky, Diffusional-thermal theory of cellular flames, Comb. Sci. Tech. 15 (1977) 137–146.

[2] G. Joulin, G. I. Sivashinsky, Influence of momentum and heat losses on the large-scale stability of quasi-2D premixed flames, Combust. Sci. and Tech. 98 (1994) 11–23.

[3] S. H. Kang, H. G. Im, S. W. Baek, A computational study of Saffman-Taylor instability in premixed flames, Combust. Theory Modelling 7 (2003) 343–363.

[4] S. H. Kang, S. W. Baek, H. G. Im, Effects of heat and momentum losses on the stability of premixed flames in a narrow channel, Combust. Theory Modell 10 (4) (2006) 659–681.

[5] V. N. Kurdyumov, M. Matalon, Flame acceleration in long narrow open channels, Proc. Combust. Inst. 34 (2013) 865–872.

[6] L. Kagan, P. Gordon, G. Sivashinsky, An asymptotic study of the transition from slow to fast burning in narrow channels, Proc. Combust. Inst. To appear.

[7] J. Gross, X. Pan, P. D. Ronney, Flame propagation at low Lewis number in narrow slots, Tech. rep., Spring Technical Meeting, Combustion Institute, Western States, Section, March 24-25, Pasadena, CA (2014).